IEEE Access
Multidisciplinary | Rapid Review | Open Access Journal

Received March 30, 2022, accepted April 25, 2022, date of publication May 4, 2022, date of current version May 13, 2022.

Digital Object Identifier 10.1109/ACCESS.2022.3172696

Home Energy Management System for Price-Responsive Operation of Consumer Technologies Under an Export Rate

PRATEEK MUNANKARMI[1], (Member, IEEE), HONGYU WU[2], (Senior Member, IEEE), ANNABELLE PRATT[1], (Senior Member, IEEE), MONTE LUNACEK[1], SIVASATHYA PRADHA BALAMURUGAN[1], AND PAUL SPITSEN[3]

[1]National Renewable Energy Laboratory, Golden, CO 80401, USA
[2]Mike Wiegers Department of Electrical and Computer Engineering, Kansas State University, Manhattan, KS 66506, USA
[3]Department of Energy Office of Energy Efficiency and Renewable Energy, Washington, DC 20585, USA

Corresponding author: Prateek Munankarmi (prateek.munankarmi@nrel.gov)

This work was supported in part by the National Renewable Energy Laboratory, Operated by Alliance for Sustainable Energy, LLC, for the U.S. Department of Energy (DOE) under Contract DE-AC36-08GO28308; in part by the U.S. Department of Energy Office of Energy Efficiency and Renewable Energy, Office of Strategic Programs; in part by the U.S. Department of Energy Office of Energy Efficiency and Renewable Energy Solar Energy Technologies Office; and in part by the U.S. Department of Energy Office of Electricity Advanced Grid Research and Development Program through the Grid Modernization Initiative.

ABSTRACT Dynamic tariffs such as time-of-use (TOU) were introduced to motivate consumers to change the operation of their behind-the-meter (BTM) resources to reduce their power consumption during peak demand times. Recently, export rates have been implemented that reimburse consumers for electricity exported to the grid at a rate less than the retail rate to reduce reverse power flow in distribution power systems with high photovoltaic penetrations. Export rates are expected to be employed more widely, and therefore it is important to understand their impact on consumers, the operation of BTM resources, and the distribution grid. This paper presents a home energy management system (HEMS) capable of optimally scheduling BTM resources under a tariff with export rates. The proposed HEMS is formulated as a multi-objective model predictive control problem. In the paper, we analyze the performance of the proposed HEMS under an export rate including the operation of each BTM resource and the impact on the cost and comfort of homeowners. We also compare the performance of the proposed HEMS under an export rate with the HEMS under a TOU rate. Simulation results are presented for a small power system with several homes that employ the proposed HEMS to respond to an export rate. The simulation results show that the estimated energy cost savings for houses with HEMS and energy storage under an export rate is 20% compared to the baseline scenario with no HEMS. The results also demonstrate that the proposed HEMS responding to an export rate increases the self-consumption of buildings more than HEMS responding to a TOU rate.

INDEX TERMS Behind-the-meter resources, co-simulation, dynamic tariff, export rate, home energy management system.

NOMENCLATURE

A. INDICES, SETS AND PARAMETERS

NT	Number of time periods
NS	Number of scenarios
T^i	Customer-specified operational time span for appliances
A	Set of controllable appliances, $A = \{\text{hvac, fr, wh, ev, bess, cwd, dw, pp}\}$
A^{th}	Set of controllable thermal appliances, $A^{th} = \{\text{hvac, fr, wh}\}$
$\Pr_s$	Occurrence probability of scenario s
$P_t^{\max}$	Maximum allowable electricity load at time
$E^{\max}$	Maximum allowable energy import from the grid across the scheduling horizon
P_i^{rate}	Rated power of appliance i

The associate editor coordinating the review of this manuscript and approving it for publication was Bin Zhou.

$\Theta_{i,t}^{\min}$, $\Theta_{i,t}^{\max}$	Min/max substance temperature set point for appliance i at time t, $i \in A^{th}$
$\Theta_{i,t}^{desired}$	Desired substance temperature controlled by appliance i at time t, $i \in A^{th}$
τ	Time interval, in hour
$\varphi_{(\cdot)}^{(\cdot)}$	Thermal coefficients
RE_i	Required energy of appliance i for a task
κ_i	Penalty factor of appliance i for substance temperature deviation from the desired temperature
$QC_i^{\min}$, $QC_i^{\max}$	Min/max charge power, $i \in \{bess, ev\}$
$QD_i^{\min}$, $QD_i^{\max}$	Min/max discharge power, $i \in \{bess, ev\}$
$SOC_i^{\min}$, $SOC_i^{\max}$	Min/max state of charge, $i \in \{bess, ev\}$
Cap_i	Capacity, $i \in \{bess, ev\}$
E_{ev}^{req}	Estimated energy requirement to reach target SOC for EV
η_i^{char}, $\eta_i^{dischar}$	Charge/discharge efficiency, $i \in \{bess, ev\}$
γ_t	Demand-response price at time t
Pen_i	Penalty associated with slack variable
λ_t^{im}	Import price at time t
λ_t^{ex}	Export price at time t

B. STOCHASTIC VARIABLES

$\hat{\Theta}_{t,s}^{out}$	Outdoor temperature at time t in scenario s
$\hat{\chi}_{t,s}$	Solar irradiance at time t in scenario s
$\hat{w}_{t,s}$	Hot water usage at time t in scenario s
$\hat{p}_{wind,t,s}$	Wind generation at time t in scenario s
$\hat{p}_{solar,t,s}$	Solar generation at time t in scenario s
$\hat{p}_{ncl,t,s}$	Noncontrollable loads at t in scenario s

C. VARIABLES

$I_{i,t,s}$	State of appliance i at time t in scenario s; 1 for ON, otherwise 0
$\theta_{i,t,s}$	Substance temperature of thermal appliance at time t in scenario s
$\theta_{i,t,s}^{SP}$	Substance temperature set point of thermal appliance i at time t in scenario s
$DR_{t,s}$	Baseline load reduction at time t in scenario s
$p_{i,t,s}$	Electricity consumption (+) or generation (−) of appliance i at time t in scenario s
$p_{t,s}^{im}$	Power imported from grid to home at time t in scenario s
$p_{t,s}^{ex}$	Power exported from home to grid at time t in scenario s
$I_{t,s}^{im}$	Import state of HEMS at time t in scenario s; 1 for import, otherwise 0
$I_{t,s}^{ex}$	Export state of HEMS at time t in scenario s; 1 for export, otherwise 0
$SOC_{(\cdot),t,s}$	SOC of BESS/EV at time t in scenario s
$Slack_{i,t,s}$	Nonnegative slack variable for appliance i at time t in scenario s, $i \in \{ev, cwd, dw, pp\}$

I. INTRODUCTION

Distributed solar photovoltaic (PV) system deployment in residential, commercial, and industrial buildings is expected to continue to increase at a rapid pace, and this will result in significant changes in power systems. The International Energy Agency (IEA) forecasts global distributed PV capacity to more than double in the next 5 years through an expected increase of 320 GW to total more than 500 GW [1]. This increase is primarily driven by continued projected PV cost reductions [1], with PV levelized costs in 2023 forecast to be three to seven times lower than in 2011, depending on the location [1]. Retail electricity prices, remuneration schemes for excess generation, and economic incentives are other important factors that determine the economic attractiveness of distributed PV for consumers [2]. An increased focus by distribution system operators on improving the resilience of distribution systems and increasing the efficiency of energy delivery is also expected to contribute to increased distributed generation [3]. Electric utilities and policymakers worldwide are facing new opportunities and challenges as consumers generate a larger share of their electricity [1]. High penetrations of distributed PV can challenge electric utilities with overvoltages and voltage variability, reverse power flow, increased reactive power requirements, and difficulty in islanding detection [3]. Such challenges have traditionally been addressed through infrastructure upgrades.

An alternative to feeder upgrades to address some of these challenges is the operational management of behind-the-meter (BTM) resources—such as battery energy storage systems (BESS); electric vehicles (EVs); smart PV systems; and responsive load, including water heaters and air conditioners—with a home energy management system (HEMS). This approach requires building owners to be provided with appropriate financial incentives to support the distribution system. Consideration of the occupants' comfort in addition to the financial incentives can ensure continued participation of building owners in the provision of grid services [4].

Buildings, especially commercial buildings, have long been engaged in providing peak load reduction services through demand-response (DR) programs, either through direct payments to consumers (incentive-based DR) for their participation or through dynamic pricing schemes to motivate consumers to change their load shape (price-based DR). Flat rate tariffs with no daily or seasonal variation, though the most widely used tariff structure for residential consumers, do not provide incentives for building owners to change the operation of their BTM resources [5], [6]. Empirical studies have shown that consumers can understand and respond to new tariffs with variable rates [7] and therefore dynamic pricing tariff structures—including real-time price (RTP), time-of-use (TOU) price, and critical peak price—are being implemented for price-based DR schemes [8]. By 2014, utilities in 49 states of the United States offered some form of TOU to residential consumers [9], and by 2015, 2.2 million residential consumers were enrolled in TOU

rates [10]. Currently, approximately one in seven utilities in the United States and approximately half of investor-owned utilities offer a residential TOU rate [7]. Arizona Public Service has the highest participation, with approximately 57% of residential consumers enrolled in TOU rates [7].

Feed-in tariffs (FiT) provide payments (or credits) to consumers for energy generated by BTM renewable generation. They were introduced to encourage the deployment of renewable energy technologies [11]. Recent reductions in FiT in countries such as Germany [12] and the United Kingdom [13] encourage self-consumption for residential consumers. Net metering schemes, in which consumers receive retail rates for electricity exported to the grid, have become more common, and it is expected that one-third of the distributed PV capacity forecast to come online by 2023 globally will operate under net metering schemes [2].

More recently, export (or two-way) rates have been introduced in large part to address reverse power flow in areas of high PV penetration. An export rate is used within a tariff structure to reimburse consumers for electricity exported to the grid. The rate for export to the grid is typically lower than the rate for import from the grid, thereby motivating consumers to self-consume excess PV production. The smart export guarantee is a legal obligation in the United Kingdom, implemented in Jan. 2020, that requires energy suppliers that have more than 150, 000 customers to offer at least one export tariff [14], [15]. Similarly, some utilities in the United States, such as Arizona Public Service, are implementing export rates [16]. It has been recognized that consideration of more complex rates requires a greater understanding of the potential impacts [7]; therefore, as export rates become more common, it is important for electric utilities and policymakers to understand the impacts of tariffs with export rates on consumers, the operation of BTM resources, and the distribution system.

A. LITERATURE REVIEW

In recent years, there have been several discussions in the literature regarding the various rate structures and consumer responses to these rates. It has also been recognized that smart technologies, such as smart thermostats and HEMS, can contribute to the success of dynamic pricing case studies [7].

The design of fair and reasonable FiT rates is discussed in [17]. In [18], an economic and technical analysis of a state-of-charge (SOC) rule-based energy management system is presented for the operation of a battery under a FiT. Similarly, the authors in [6] proposed an optimization model for the optimal operation of a PV-battery system under a FiT, and they performed a sensitivity analysis on the impact of battery capacity on the model. Methods for determining the optimal size of a PV-battery system under different tariffs have been developed. For example, [19] proposed a particle-swarm optimization algorithm under a FiT for South Australia, whereas [20] proposed a mixed integer linear programming (MILP) optimization algorithm under a TOU tariff with demand charges.

Various algorithms for HEMS responding to TOU rates have been proposed in the literature. A review of demand-side management schemes, including HEMS-based demand-side management under various pricing tariffs—including fixed tariff, TOU, RTP, and inclined block rate—was discussed in [21]. It is noteworthy that HEMS under an export rate has not been discussed previously in the literature. A MILP optimization to schedule the smart home appliances with the objectives of minimizing the total utility cost and peak demand was proposed in [22]. A computationally efficient two-horizon method for residential energy management under a TOU rate was proposed in [23]. In [24], a dynamic programming approach was proposed to manage controllable loads as well as EVs. An approximate dynamic programming approach was employed in [25] to optimize appliance schedules while considering multiple uncertainty sources. Two partially observable Markov decision processes were proposed to manage nonthermal appliances under an RTP tariff [26].

A HEMS based on a stochastic multi-objective optimization model to optimally schedule consumer appliances in response to TOU rates or RTP, using a MILP optimization formulation, was presented in [27]. The impact of this HEMS responding to TOU rates on the operation of the distribution system was explored through software simulations in [28] and through hardware-in-the-loop simulations in [29], [30]. The authors in [31] proposed the rule-based (time-based) operation of home batteries in response to a TOU and export tariff.

A residential energy management strategy to minimize the utility cost while considering human interaction and user preferences was proposed in [32]. An energy management system to manage energy consumption within a building under a target consumption level was proposed in [33]. A unified demand-side management model to reduce electricity cost, peak load demand, and distribution losses was considered in [34]. An energy management algorithm to minimize energy consumption from the grid and to maximize the use of renewable energy in a microgrid was considered in [35]. A joint model considering energy management within a microgrid and an energy trading model among microgrids was proposed in [36].

B. MOTIVATION AND CONTRIBUTIONS

Most studies in the literature demonstrate the performance of HEMS under TOU or RTP rates. An automated HEMS capable of coordinating and controlling several BTM resources—such as a BESS, air conditioner, water heater, and an EV—under an export rate has not been reported.

In this work, we propose a HEMS capable of optimizing the operation of multiple consumer appliances—including a BESS, EV, and smart thermostats coupled with air conditioners and electric resistance water heaters—under an export rate. The proposed HEMS is formulated as a stochastic multi-objective model predictive control (MPC) problem. The objective of the HEMS is to minimize the weighted

sum of energy cost, thermal discomfort, and total and peak electricity consumption. The proposed HEMS is solved using a MILP solver. Though a similar MPC architecture is used in the authors' previous work [27], the optimization model itself is entirely reformulated in this work to enable the HEMS to operate under an export tariff.

We present simulation results from a small distribution system with multiple homes to demonstrate the performance of the proposed HEMS under an export tariff. We also present results of this system with HEMS under a TOU tariff to understand the differences in the operation of consumer technologies under various tariff designs.

The main contributions of this work are as follows:

- Develop a HEMS optimization model for effectively scheduling the operations of BTM resources under an export rate.
- Present analysis of the performance of the proposed HEMS under an export rate, including the operation of each BTM resource.
- Compare the impact of HEMS under an export tariff with HEMS under a TOU tariff and a baseline scenario without HEMS. The results demonstrate the increase in self-consumption when HEMS respond to an export rate compared to when HEMS respond to a TOU rate.

The rest of the paper is organized as follows. Section II presents the detailed formulation of a HEMS that can respond to an export rate. Section III describes the co-simulation platform used to generate the simulation results. Section IV outlines the various scenarios and simulation parameters used for the case study. Section V presents the simulation results for HEMS operating under TOU and export tariff structures. Finally, section VI presents the concluding remarks.

II. HEMS FORMULATION FOR EXPORT RATE

In this section, we present the mathematical formulation of a HEMS capable of responding to an export rate under uncertainties in outdoor temperature, renewable energy generation, water usage, and non-controllable loads. Without loss of generality, we model the HEMS by using stochastic programming that explicitly incorporates a probability distribution of the uncertainty and relies on presampling scenarios, each representing a possible realization of the uncertainties with a preassigned occurrence probability. A conceptual diagram of the HEMS is shown in Fig. 1.

A. HEMS OBJECTIVE FUNCTION

The HEMS formulation with the export rate encompasses the following objectives, representing a variety of needs by the utilities and/or residential customers:

1) **Thermal discomfort**, which is modeled as a linear penalty function (1) for the expected substance temperature deviation from the customer's desired temperature:

$$J_1 = \sum_{s=1}^{NS} \Pr_s \cdot \sum_{i \in A^{th}} \sum_{t=1}^{NT} \kappa_i \cdot |\Theta_{i,t}^{desired} - \theta_{i,t,s}| \quad (1)$$

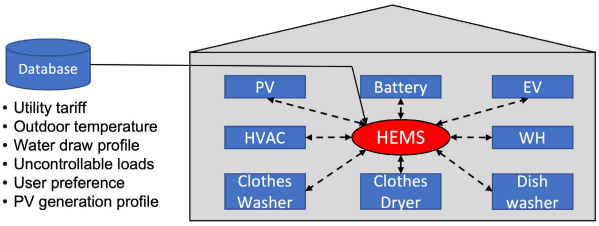

FIGURE 1. Conceptual diagram of HEMS controlling BTM resources.

2) **Total energy cost ($)**, which represents the expected cost of the electricity consumption under the export rate and the revenue received from participating in an incentive-based DR program (2):

$$J_2 = \sum_{s=1}^{NS} \Pr_s \cdot \sum_{t=1}^{NT} \tau \cdot (p_{t,s}^{im} \cdot \lambda_t^{im} - p_{t,s}^{ex} \cdot \lambda_t^{ex} - DR_{t,s} \cdot \gamma_t) \quad (2)$$

3) **Total electricity consumption (kWh)**, which consists of the expected electric energy consumption of all appliances over the entire scheduling horizon (3):

$$J_3 = \sum_{s}^{NS} \Pr_s \cdot \sum_{t=1}^{NT} \tau \cdot (\sum_{i \in A} p_{i,t,s} + \hat{p}_{ncl,t,s}) \quad (3)$$

4) **Peak electricity power (kW)**, which represents the expected peak electricity consumption during the scheduling horizon (4):

$$J_4 = \sum_{s=1}^{NS} \Pr_s \cdot \max\{p_{1,s}^{im}, p_{2,s}^{im}, \ldots, p_{NT,s}^{im}\} \quad (4)$$

The peak power is identified as the upper bound on the imported electricity under the export rate. The peak power is important to commercial buildings because utilities often charge businesses based on the peak demand during a billing period. For residential customers subject to peak charges, minimizing the maximum imported electricity by optimally managing all the controllable devices could reduce their energy bills. Note that this objective is usually minimized in conjunction with other objectives, such as (1) and (2).

Because of these objectives, it is imperative to construct an objective function such that residential customers' preferences are satisfied by HEMS; therefore, a linear scalarization technique with normalization is employed to convert the multiple objectives into a single objective function with residential customers' preferences as a priori [27]. Specifically, any combination of these objective components through a weighted average becomes the overall objective function (5) as follows:

$$\begin{aligned} Minimize\ J = {} & \alpha_1 \cdot J_1/\tilde{J}_1 + \alpha_2 \cdot J_2/\tilde{J}_2 \\ & + \alpha_3 \cdot J_3/\tilde{J}_3 + \alpha_4 \cdot J_4/\tilde{J}_4 \end{aligned}$$

$$+ \sum_{i\in\{ev,cwd,dw,pp\}} \sum_{t=1}^{NT} \sum_{s=1}^{NS} Pen_i \cdot Slack_{i,t,s} \quad (5)$$

In (5), decision variables can be found in (1)–(4); $\tilde{J}_1, \tilde{J}_2, \tilde{J}_3$, and $\tilde{J}_4$ are the upper bounds of the corresponding objective components from (1)–(4), which are estimated by a computationally efficient normalization method to combine different objective components [27]. Specifically, if the user-specified preference is identified as a multi-objective optimization—e.g., when J_1 and J_2 are considered simultaneously—the deterministic model with the forecast of stochastic parameters is run with the integer variables relaxed, and the resulting optimization problem is solved by using linear programming with a negligible computational effort. The objective of the first deterministic run is to minimize the total energy cost, J_2, such that the upper bound of the thermal discomfort, i.e., $\tilde{J}_1$, is obtained. Then, with a trivial computational overhead, the deterministic model is executed again with the objective of minimizing J_1, such that $\tilde{J}_2$ is determined. $\tilde{J}_3$ and $\tilde{J}_4$ can be accurately estimated based on historical data. In (5), because the units of $\tilde{J}_1, \tilde{J}_2, \tilde{J}_3$, and $\tilde{J}_4$ are, respectively, identical to those of J_1, J_2, J_3, and J_4, the coefficients $\alpha_1, \alpha_2, \alpha_3$, and α_4 are unitless, representing the customers' preference known a priori. The summation of those coefficients equates to 1.

Slack variables are introduced into the model, as seen in the third line of (5), to provide the HEMS with more flexibility by allowing some constraints (e.g., EV SOC requirement at departure) to be violated at an extremely high penalty cost. The proposed HEMS model for the export rate minimizes the weighted average of multiple objective components while aiming to satisfy the operational constraints, which are described in the next section II-B.

B. HEMS CONSTRAINTS

Both house-wide and appliance-level constraints are included in the HEMS formulation, as described in this section. Appliance-level constraints are included for a heating, ventilation, and air-conditioning (HVAC) system; refrigerator; water heater; dishwasher; clothes washer and dryer; pool pump; BESS; and EV. The HEMS can also incorporate a micro-combined-heat-and-power (CHP) model, in which the CHP's constraints include the CHP operational constraint, power output limit, heating output limit, and natural gas consumption constraint [27]. In such a case, the gas price and CHP gas consumption should be considered in the energy cost component (2) of the overall objective function.

1) HOUSE-WIDE CONSTRAINTS

The house-wide constraints are formulated in (6)–(8). Constraint (6) describes the relationship between the appliance and noncontrollable load powers and the import and export powers. This constraint guarantees that the electricity generation and load are balanced at time t, where nonnegative variables $p^{im}_{t,s}$ and $p^{ex}_{t,s}$ represent the power imported from and exported to the grid, respectively. The two variables are determined by the appliance power consumption, $p_{i,t,s}$, in (6), where the temperature set points and ON/OFF status of the appliances and the BESS/EV charge/discharge set points are highly coupled.

Constraint (7) ensures that the maximum electricity extracted from the grid at any given time period should not exceed a specified value. This constraint is formulated for customers who enroll in a DR program in response to utilities' power-reduction requests during some critical time periods, such as summer peaks. Constraint (8) indicates that the total energy drawn from the grid should not exceed a predefined value. The appliance scheduling of a net-zero energy house [37], [38] can be obtained by setting $E^{\max} = 0$ in a long-term operation, indicating that the total energy consumption is equal to the energy generated by the on-site renewable energy sources:

$$p^{im}_{t,s} + \hat{p}_{solar,t,s} + \hat{p}_{wind,t,s} = \sum_{i\in A} p_{i,t,s} + \hat{p}_{ncl,t,s} + p^{ex}_{t,s}, \quad \forall t,\ \forall s \quad (6)$$

$$p^{im}_{t,s} \le P^{\max}_{t}, \quad \forall t,\ \forall s \quad (7)$$

$$\sum_{t=1}^{NT} (p^{im}_{t,s} - p^{ex}_{t,s}) \cdot \tau \le E^{\max}, \quad \forall s \quad (8)$$

2) POWER IMPORT AND EXPORT CONSTRAINTS

The HEMS import and export constraints interacting with the power grid are listed in (9)–(12). Constraint (9) guarantees that the power import and export are mutually exclusive at any time period and thus cannot occur simultaneously. Constraint (10) indicates there is no power export to the grid when the import state indicator is equal to 1. Conversely, constraint (11) suggests there is no power import from the grid when the export state indicator is 1. Constraint (12) ensures there is neither import nor export if both indicators are equal to 0, i.e., the home is in an islanding mode. In (10)–(12), M is a large positive constant.

$$I^{im}_{t,s} + I^{ex}_{t,s} \le 1 \quad (9)$$

$$p^{ex}_{t,s} \le M \cdot (1 - I^{im}_{t,s}) \quad (10)$$

$$p^{im}_{t,s} \le M \cdot (1 - I^{ex}_{t,s}) \quad (11)$$

$$p^{im}_{t,s} + p^{ex}_{t,s} \le M \cdot (I^{im}_{t,s} + I^{ex}_{t,s}) \quad (12)$$

3) THERMODYNAMIC MODELS OF HVAC, REFRIGERATOR, AND WATER HEATER

We employ a first-order thermodynamic model widely used in the literature [27], [30], [39]. For the HVAC system, this model considers the evolution of the room temperature, $\theta_{hvac,t,s}$, as a function of the temperature at the previous time, the power consumed by the HVAC, the outdoor temperature, and solar irradiance. The HVAC constraints (13)–(14) are listed as follows:

$$\Theta^{\min}_{hvac,t} \le \theta^{SP}_{hvac,t,s} \le \Theta^{\max}_{hvac,t}, \quad \forall t,\ \forall s \quad (13)$$

$$\theta_{hvac,t,s} = \begin{cases} \varphi^{rm}\theta_{hvac,t-1,s} + \varphi^{c}_{hvac}p_{hvac,t,s} + \varphi^{si}\hat{\chi}_{t,s} \\ +\varphi^{out}\hat{\Theta}^{out}_{t,s}\ ,\ \forall t, \forall s, \quad \textit{if cooling} \\ \varphi^{rm}\theta_{hvac,t-1,s} + \varphi^{h}_{hvac}p_{havc,t,s} + \varphi^{si}\hat{\chi}_{t,s} \\ +\varphi^{out}\hat{\Theta}^{out}_{t,s}\ ,\ \forall t, \forall s, \quad \textit{if heating} \end{cases} \tag{14}$$

Constraint (13) shows that the cooling or heating set points should be within their respective ranges prescribed by the residential customer. Constraint (14) represents the thermal dynamics of the room temperature in both cooling (c) and heating (h) modes. The heating or cooling mode is selected by the user, i.e., a priori to the model. In (14), φ^{rm}, φ^{si}, and φ^{out} denote the thermal coefficients with respect to room, solar irradiance, and outside, respectively; φ^{c}_{hvac} and φ^{h}_{hvac} account for the cooling and heating efficiency (including the coefficient of performance) of the HVAC, respectively; other thermal coefficients, $\varphi^{(\cdot)}$, can be calculated based on the thermal capacitance and resistance of the house. Here, the cooling or heating set points are the only decision variables of the HVAC; other variables, such as the ON/OFF status and power consumption, are associated with the set points by using nested logic constraints [27].

The thermodynamic model for a refrigerator is formulated similarly to the HVAC when cooling. The difference is that the term of the solar irradiance is dropped, and the stochastic parameter, $\hat{\Theta}^{out}_{t,s}$, is replaced with the room temperature. Analogously, the cooling set point of the refrigerator is the decision variable with which the ON/OFF status and power consumption are associated by using the same method as in modeling the HVAC system.

The operational constraints of the water heater (WH) (15)–(16) are listed as follows:

$$\Theta^{\min}_{wh,t} \le \theta^{SP}_{wh,t,s} \le \Theta^{\max}_{wh,t}, \quad \forall t,\ \forall s \tag{15}$$

$$\theta_{wh,t,s} = \varphi^{tk}\theta_{wh,t-1,s} + \varphi^{usg}\hat{w}_{t,s} + \varphi_{wh}p_{wh,t,s} + \varphi^{ab}\theta^{ab}_{t,s}, \quad \forall t,\ \forall s \tag{16}$$

In (16), φ^{tk}, φ^{usg} and φ^{ab} represent the thermal coefficients associated with the water tank, hot water usage, and ambient temperature, respectively; φ_{wh} takes into account the water heater efficiency (including the coefficient of performance). The water heater ambient temperature is approximated as the average temperature between the room temperature and outside temperature (17):

$$\theta^{ab}_{t,s} = 1/2 * (\theta_{hvac,t,s} + \hat{\Theta}^{out}_{t,s}), \quad \forall t,\ \forall s \tag{17}$$

Analogously, the heating set point of the water heater is the decision variable, whereby its ON/OFF status and power consumption are determined.

Instead of the substance temperature limitation constraints, the heating or cooling set points of the HVAC, refrigerator, and water heater are constrained within the user-specified upper and lower bounds of the substance temperature. This allows the substance temperatures to go beyond the upper and lower bounds, providing greater flexibility of the house thermal storage.

4) DISHWASHER, CLOTHES WASHER AND DRYER, AND POOL PUMP MODELS

Other controllable appliances studied in this paper are interruptable appliances, including a dishwasher, clothes washer and dryer, and pool pump, whose operations can be interrupted and resumed later by the HEMS. In general, residential customers merely care about a timely completion of the function performed by those controllable appliances. The operational constraints for the dishwasher, clothes washer and dryer, and pool pump include state transition constraints (18) and (19), a power limit (20), and an energy requirement constraint (21). In (18) and (19), $x_{i,t,s}$ and $y_{i,t,s}$ are the startup and shutdown indicators, respectively. Constraint (18) states the correlation between the appliance's ON/OFF state and its startup and shutdown indicators. Constraint (19) imposes limits on the startup and shutdown operations. Constraint (20) shows that the power consumption of the appliance must be within its rated power. Constraint (21) indicates that the energy required for the appliance to complete a task must be satisfied by the HEMS. Other constraints include minimum up-/down-time constraints [3].

$$x_{i,t,s} - y_{i,t,s} = I_{i,t,s} - I_{i,t-1,s}, i \in \{pp, dw, cwd\}, \quad \forall t \in T^i,\ \forall s \tag{18}$$

$$x_{i,t,s} + y_{i,t,s} \le 1, i \in \{pp, dw, cwd\}, \quad \forall t \in T^i,\ \forall s \tag{19}$$

$$0 \le p_{i,t,s} \le I_{i,t,s} \cdot P^{rate}_{i}, \quad i \in \{pp, dw, cwd\},\ \forall t \in T^i,\ \forall s \tag{20}$$

$$\sum_{t \in T^i} (p_{i,t,s} + Slack_{i,t,s}) \cdot \tau = RE_i, i \in \{pp, dw, cwd\}, \quad \forall s \tag{21}$$

5) BATTERY ENERGY STORAGE SYSTEM MODEL

The residential BESS constraints include charge/discharge rate limits, SOC dynamics, SOC limits, and limits on initial/final SOC, which are given in (22)–(25), respectively. In (22), $p_{bess,t,s}$ is positive when charging, negative when discharging, and 0 when the storage is idle. Constraint (25) suggests that, if necessary, the storage follows a daily cycle when the SOC at the last period (t=NT) would be equal to that of the initial time in the scheduling horizon (t=0):

$$p_{bess,t,s} \in \{0, [-QD^{\max}_{bess}, -QD^{\min}_{bess}], [QC^{\min}_{bess}, QC^{\max}_{bess}]\}, \quad \forall t,\ \forall s \tag{22}$$

$$SOC_{bess,t,s} = \begin{cases} SOC_{bess,t-1,s} + p_{bess,t,s} \cdot \eta^{char}_{bess}/Cap_{bess}, \\ \qquad\qquad p_{bess,t,s} > 0 \\ SOC_{bess,t-1,s} + p_{bess,t,s}/\eta^{dischar}_{bess}/Cap_{bess}, \\ \qquad\qquad p_{bess,t,s} < 0 \end{cases} \tag{23}$$

$$SOC^{\min}_{bess} \le SOC_{bess,t,s} \le SOC^{\max}_{bess}, \quad \forall t,\ \forall s \tag{24}$$

$$SOC_{bess,0,s} = SOC_{bess,T,s}, \quad \forall s \tag{25}$$

6) ELECTRIC VEHICLE MODEL

The EV's constraints are similar to the BESS constraints (22)–(24), except that its operational time period, i.e., T^{ev}, is determined by the estimated arrival and departure time. In addition, constraint (26) ensures that the EV's energy requirement is satisfied:

$$\sum_{t \in T^{ev}} (p_{ev,t,s} + Slack_{ev,t,s}) \cdot \tau \geq E_{ev}^{req}, \quad \forall s \qquad (26)$$

where E_{ev}^{req} is the energy required to charge the EV. E_{ev}^{req} can be estimated by calculating the difference between the EV's arrival SOC and the desired departure SOC specified by the customer. To guarantee the feasibility of the HEMS model, we introduce non-negative $Slack_{ev,t,s}$ into (26), which allows the EV SOC requirement upon departure to be relaxed at the cost of a high penalty (discomfort). To correctly calculate the energy requirement in the MPC-based weekly or monthly simulation, five charging cases are considered, each of which represents one possible correlation among the initial, arrival, and departure SOC. In addition, the estimated costs of the battery degradation are captured through a piecewise linear penalty function based on a linearization of the model proposed in [40], which estimates both energy capacity fade and power fade and includes the effects caused by temperature and SOC changes. This cost can be captured in the energy cost component (2) of the overall objective function. Note that both BESS and EV can be discharged to export to the grid as deemed necessary by the HEMS.

7) STOCHASTIC APPLICATION

A HEMS model for the optimal schedules of residential appliances under export rates is formulated as a MILP problem in (1)–(26). The proposed HEMS model can be used either in a deterministic or a stochastic manner. When it is used deterministically, the forecasts of the stochastic variables (e.g., outside temperature, solar irradiance, hot water draw) are accounted for in a single-scenario optimization, the co-simulation results of which will be discussed in the next section.

When the proposed HEMS model is used stochastically, multiple scenarios need to be generated based on the forecasts of the stochastic variables, and a scenario reduction method might be used to find a trade-off between the solution accuracy and speed [41]. In such a case, first- and second-stage decision variables can be efficiently embedded in the proposed HEMS model. For example, the ON/OFF decisions of the pool pump, dishwasher, and clothes washer and dryer in the binding interval of the MPC is a first-stage, here-and-now decision, which is identical among the scenarios represented in (27) as follows:

$$I_{i,t,s} = I_{i,t}, i \in \{pp, dw, cwd\}, \quad \forall t \in T_B, \ \forall s \qquad (27)$$

where $I_{i,t}$ is the implementable of $I_{i,t,s}$ regardless of scenarios, and T_B denotes the binding interval of the MPC. Other first-stage decisions associated with each appliance can be analogously constrained. In contrast, the decisions pertaining to the look-ahead intervals (denoted by T_L) are second-stage, wait-and-see decisions, which might differ among scenarios to accommodate the forecast error. The stochastic application of the HEMS model, however, is out of the scope of this paper and warrants further examination in the future.

III. CO-SIMULATION PLATFORM

We use a modified version of the Integrated Energy System Model (IESM) co-simulation platform to perform the software simulations to evaluate the operation of the HEMS under TOU and export rates, as shown in Fig. 2. The IESM integrates the simulation of a distribution feeder, distributed energy resources (DERs) (including PV and battery systems), buildings (including building appliances and building thermal performance), and HEMS under different markets or tariff structures through a co-simulation coordinator coded in Python [30].

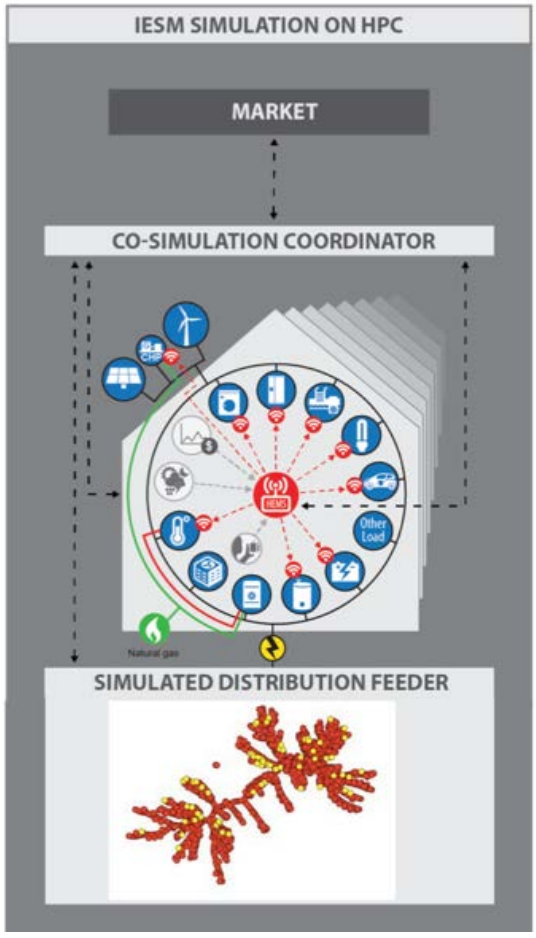

FIGURE 2. Diagram of the IESM, including a co-simulation coordinator, simulated distribution feeder, simulated homes with HEMS, and markets.

The co-simulation coordinator manages the exchange of data between the different components and the timing of the execution of all the components with varying time steps. It therefore interfaces with the distribution feeder simulation, building simulations, the HEMS, and the market that sets the

different tariff structures. The different components of the simulation are described in more detail in [30]. The simulations are performed using high-performance computing to allow for future simulations of larger systems with hundreds of houses and HEMS using an MPC approach.

The co-simulation workflow showing the interaction between the HEMS and the house models is presented in Fig. 3. We used the house model in GridLAB-D to represent the building envelope and appliance models. The co-simulation workflow is described in Algorithm 1, where an upper bar associated with a variable signifies the variable's initial value given at a specific time, an asterisk pertaining to a variable indicates its optimal value obtained from the proposed HEMS optimization, and a variable whose subscript, s, is dropped indicates its corresponding implementable regardless of scenarios.

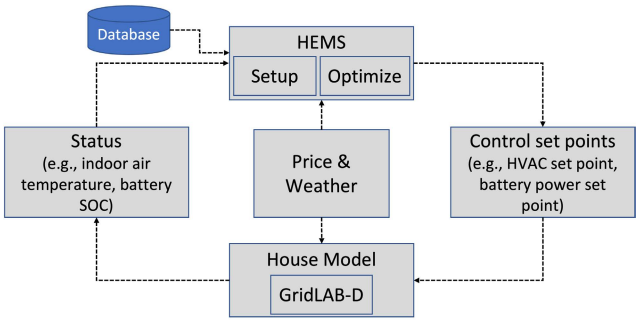

FIGURE 3. Co-simulation flowchart depicting the interaction between HEMS and the house model.

Algorithm 1: Co-Simulation Algorithm

1: At time t, receive the forecast data ($\hat{\lambda}_{t,0}$, $\hat{\Theta}^{out}_{t,0}$, $\hat{w}_{t,0}$, $\hat{p}_{solar,t,0}$, $\hat{p}_{ncl,t,0}$, $\forall t \leq T_B + T_L$) and initial status of house ($\bar{p}_{i,0}$, $\forall i \notin A^{th}$ and $\bar{\theta}_{i,0}$, $\forall i \in A^{th}$) in HEMS
2: Perform MPC optimization in HEMS to compute optimal set points for BTM resources ($\bar{p}^{*}_{i,t}$, $\bar{\theta}^{SP*}_{i,t}$, $\forall t \in T_B$ and $\bar{p}^{*}_{i,t,s}$, $\bar{\theta}^{SP*}_{i,t,s}$, $\forall t \in T_L$)
3: Send the optimal set points ($p_{i,t} = \bar{p}^{*}_{i,t}$, and $\theta^{SP}_{i,t} = \bar{\theta}^{SP*}_{i,t}$, $\forall t \in T_B$) from HEMS to house model
4: Run the house model with set points from HEMS
5: Send the initial status from house model to HEMS
6: Let $t = t + 1$; go to 1 until $t = NT$

IV. SCENARIO DEFINITION

A scenario was created for a hypothetical distribution feeder in the state of Arizona in the southwestern United States. The distribution feeder is based on the IEEE 13-node test feeder, and approximately 3% of the load is replaced with 12 houses using GridLAB-D house models randomly selected from those developed for the National Institute of Standards and Technology Transactive Energy Challenge [42]. These house models have different combinations of attributes, such as square footage and insulation. We added a 3.44-kW rooftop PV system to each house that provides on average 83% of the total energy consumed by the house loads during the simulation time period. We also add a 5-kW/13.5-kWh BESS to each house. The houses are connected through three 25-kVA, single-phase, center-tapped transformers, each serving four houses. We used typical weather data for Phoenix, Arizona, for a full week in the spring for the month of April when air conditioning use is high but not nearly continuous, as would be the case on a typical summer day. The outdoor temperature and solar insolation are shown in Fig. 4.

Although the HEMS can accommodate several different objectives and combinations of objectives, as described in Section II, results are presented here for the HEMS set to minimize the house's energy cost, with $\alpha_2 = 1$ and $\alpha_1, \alpha_3, \alpha_4 = 0$, to present a simpler comparison. Further, although the HEMS is formulated as a stochastic optimization, no uncertainties are considered in the simulations, so a deterministic optimization is performed. Similarly, the HEMS formulations were developed with the ability to manage many different household appliances, but for this study, the HEMS control only the thermostat set points for the air conditioners and electric water heaters and the charge and discharge rates for the BESS. The air conditioner and water heater in the houses are modeled explicitly, and the rest of the household loads are modeled as a lumped ZIP load with a time-varying base power profile. The desired air and water temperature profiles are set to constant values. The desired temperatures for each house are different, varied uniformly between 70°F and 75°F for the air temperature and between 120°F and 140°F for the water temperature. A randomized water draw profile from [42] is used for each home. Each HEMS uses MPC to adjust the cooling set point from the desired temperature to minimize cost. The HEMS is allowed to adjust the air temperature set points up to 2.5°F above or below the desired air temperature and up to 10°F above or below the desired water temperature. This allows the air to be precooled and the water to be preheated before peak electricity prices. The battery end SOC constraint is set to 50% in the HEMS. The HEMS optimizations are performed every 15 minutes using the Gurobi 8.1 solver.

We use retail electricity rates that are currently in place for households in Arizona. The TOU rate has a varying electricity price with peak and off-peak rates. The summer peak and off-peak rates are 23.068 c/kWh and 10.873 c/kWh, respectively. Summer peak hours are from 3:00 PM to 8:00 PM, Monday through Friday [16]. All weekend hours are off-peak, but for illustrative purposes, we apply TOU rates to all days. The TOU rate structure is shown in Fig. 4. For TOU, we assume net metering and that the houses are compensated for export power at the TOU rate. The export rate is the same for consumption, but it compensates houses for export power at only 2.989 c/kWh and 2.897 c/kWh, respectively, during peak and off-peak hours [16].

We simulated three scenarios. The first is baseline operation with no price-responsive control, i.e., no HEMS. We keep

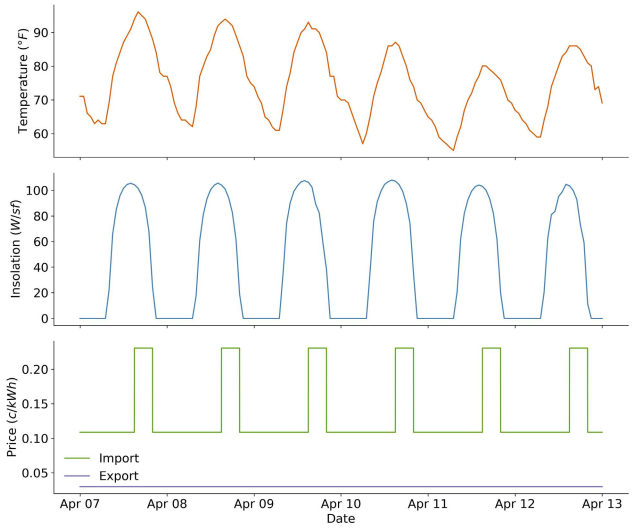

FIGURE 4. Simulation inputs including outdoor temperature (top), solar insolation (second from top), import price used for the TOU and export rate cases (bottom), and export price used for the export rate case (bottom).

the BESS in an idle mode in the baseline scenario because some form of control is required to operate the BESS, which results in price-responsive behavior. The second is a scenario where each house has a HEMS, using the formulation provided in [27], under the TOU rate with net metering. Third, we simulate a scenario where each house has a HEMS, using the formulation developed in this paper, and a BESS, under the export rate. Under the export rate structure, the export power is compensated at the export rate, whereas the power consumption is charged at the TOU rate.

V. RESULTS

First, we consider the impact on consumer energy cost, and then we evaluate the changes in household power consumption and the resulting impact on consumer comfort based on air temperature and hot water temperature. We also examine the BESS behavior and changes in operation of the water heaters and air conditioners.

A. UTILITY COST

Fig. 5 shows a violin plot indicating the distribution of the electricity expenses for the households. A violin plot is similar to a box plot with the addition of a rotated kernel density plot. A small white dot in each violin represents the median value (utility cost in this case), and the black vertical box represents the interquartile range (1^{st} and 3^{rd} quartile ranges). The broader section in each violin represents a higher probability of occurrence, whereas a narrower section represents a lower probability.

The utility cost varies because of variations in the desired air and hot water temperatures among houses as well as variations in house attributes. Baseline operation with no HEMS and no BESS results in the same power consumption for each house, but their expenses differ because of the different rates that are applied. For the time period analyzed, the expenses for households under the export rate are significantly higher than those under the TOU rate for the baseline operation. This is because all the houses have rooftop PV systems and the houses export power during times of high PV generation. Under the TOU rate, they are credited for those exports at a much higher rate, 23.068 c/kWh, than under the export rate, which credits exports at only 2.989 c/kWh. Households operating with a HEMS and a BESS under the TOU tariff have the lowest expenses, and some of them even earn income from the utility. This is mainly because these houses take advantage of the high credit for exported power during the peak TOU rate period by discharging their batteries during that time, as is discussed in more detail in Section V-B. Houses that operate with a HEMS and a BESS under both the TOU rate and the export rate are also able to reduce their expenses compared to their respective baseline operations by shifting some of their demand for air cooling and hot water heating to fall outside the TOU peak hours. Under the export rate, bills are approximately 20% less when HEMS and BESS are used. Under the TOU rate, households change from paying a modest amount on average to earning a modest credit.

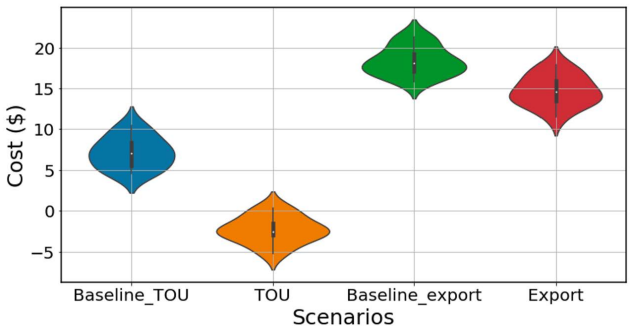

FIGURE 5. Distribution of consumer electricity bills during the time period April 7–12.

B. HOUSE LOAD PROFILE

Fig. 6 shows the average daily profile of the power drawn from the grid by the houses. In this and other figures, the solid lines display the mean over all the houses and over all 6 days, calculated at 5-minute intervals; and the shaded areas around the solid lines indicate the 5% to 95% quartile range of the data. Vertical dotted lines in this and other figures indicate the start and end of the peak pricing time periods. Similarly, the legends in the figures represent the scenarios described in Section IV. Fig. 7 shows the average daily profile of the power that is exported from the houses to the grid.

Houses operating with a HEMS and a BESS under both the TOU and the export rate have less export power than the baseline during the off-peak price period with PV production because the HEMS charges the batteries during these times. This can be observed by considering Fig. 8, which shows the average daily profile of the PV generation and the battery

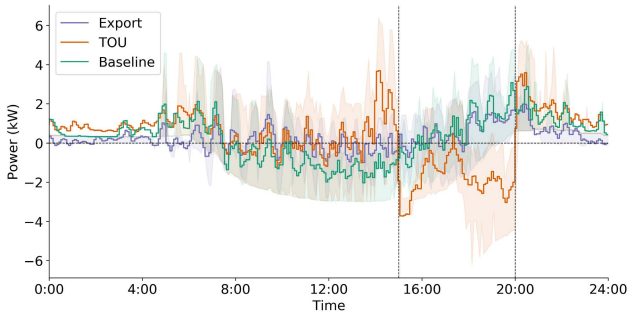

FIGURE 6. Average daily profile of house power for baseline operation, operation with BESS and HEMS responding to a TOU rate, and operation with BESS and HEMS responding to an export rate.

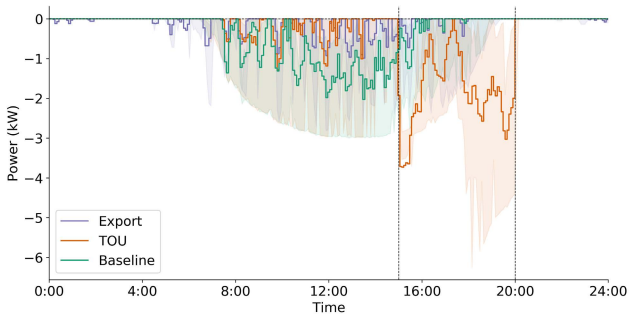

FIGURE 7. Average daily profile of power exported by houses for baseline operation, operation with BESS and HEMS responding to a TOU rate, and operation with BESS and HEMS responding to an export rate.

power, and Fig. 9, which shows the average daily profile of the battery SOC. Houses operating with a HEMS and a BESS under the TOU rate export more power than the baseline during the peak-price period because the HEMS discharges the batteries during this period to provide income to the homeowner. HEMS in houses operating under the export rate discharge the batteries to minimize the grid import because the cost of power imported from the grid is higher than the credit gained for power exported to the grid.

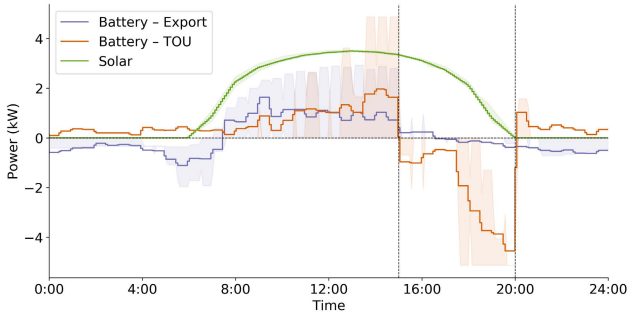

FIGURE 8. Average daily profile of PV generation and battery power for operation with HEMS responding to a TOU rate and an export rate.

These responses by the HEMS under different rate structures lead to differences in self-consumption. We calculate a self-consumption metric (γ), defined in (28), that shows

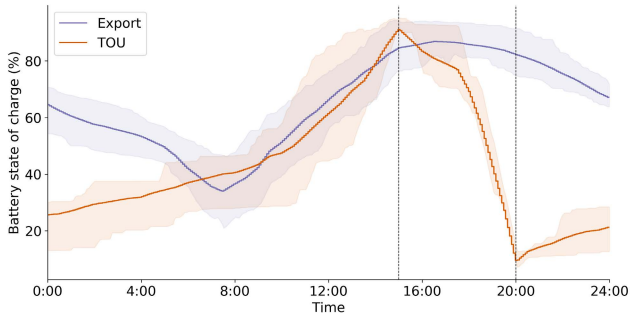

FIGURE 9. Average daily profile of battery SOC for operation with HEMS responding to a TOU rate and an export rate.

the fraction of the total energy demand of the house loads, E_{demand}, met by BTM generation sources.

$$\gamma = \frac{(E_{demand} - E_{import})}{E_{demand}} \tag{28}$$

where E_{import} represents the total energy imported from the grid. Table 1 shows the total house load and total imported energy averaged per house as well as the self-consumption metric. Self-consumption is highest in the case of HEMS operating under an export rate because lower compensation for export energy motivates the HEMS to maximize self-consumption. Similarly, self-consumption is lowest in the case of HEMS operating under a TOU rate because houses with HEMS export more energy during the peak-price period to provide financial benefit to the consumer.

TABLE 1. Self-consumption metric for different scenarios.

	$E_{demand}(kWh)$	$E_{import}(kWh)$	γ
Baseline	290.13	168.18	0.42
TOU	280.56	204.17	0.27
Export	277.43	134.9	0.51

In addition, the daily profile of houses with HEMS and BESS operating under the TOU rate have more variability and higher rates of change in power than for baseline operation, which is much more demanding of an electric utility. The power profile for houses with HEMS and BESS operating under an export rate are smoother than those operating under the TOU rate, which is preferred from an electric utility operator's perspective.

C. END-USE OPERATION

The HEMS aims to reduce air conditioner and water heater power consumption, especially during the peak-price period, to minimize the consumer's electricity bill. It preheats the water just before the peak-price period and allows the water temperatures to be less by approximately 5°F during off-peak times than the baseline case. This is shown in Fig. 10, which shows the hot water temperature, and Fig. 11, which shows the water heater power use. Fig. 12 shows that there

is considerable water demand during the peak-price period, which limits the power savings that can be achieved while maintaining occupant comfort.

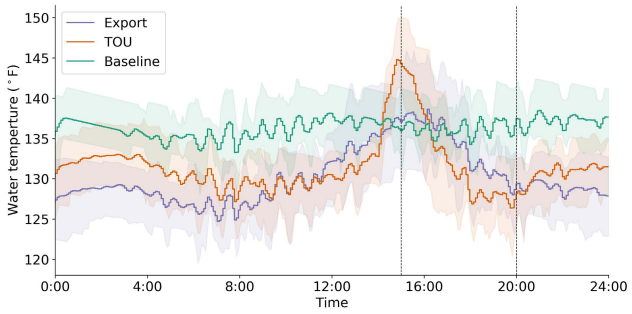

FIGURE 10. Average daily profile of hot water temperature.

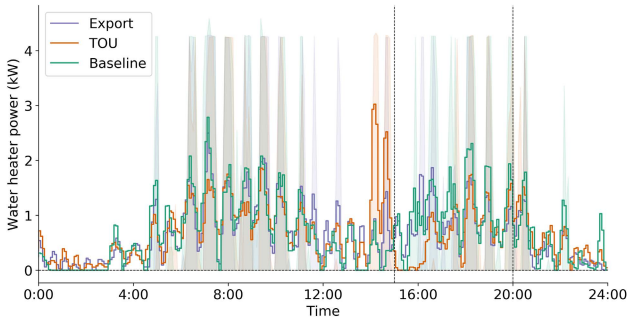

FIGURE 11. Average daily profile of water heater power.

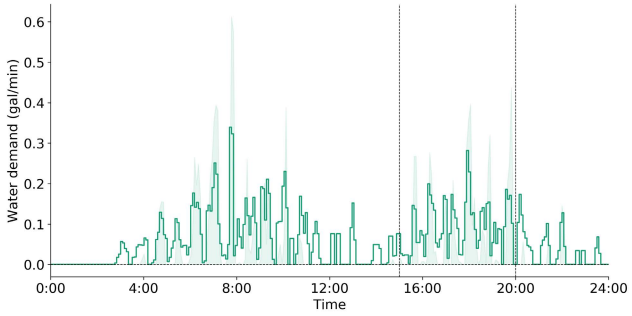

FIGURE 12. Average daily profile of water demand.

The HEMS allows the air temperatures to be higher by 1°F to 2°F than the baseline case during and after the peak-price period, as shown in Fig. 13, to reduce the air conditioner power consumption. The HEMS operating under the TOU rate precools the air prior to the peak-price period to shift power use from times when the cost is higher to earlier hours when it is not as expensive. The HEMS operating under the export rate sets the air temperature to be higher across the entire time that the air conditioner operates. The TOU strategy results in more cost savings.

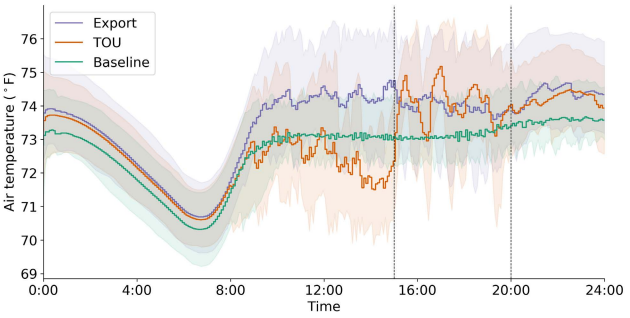

FIGURE 13. Average daily profile of indoor air temperature.

VI. CONCLUSION

This paper presents the formulation of a HEMS that can optimize the operation of home appliances under an export rate. The performance of the HEMS under an export rate describing the detailed operation of each BTM resource and the impacts on consumer cost and comfort is analyzed in the paper. We also compare the performance of the HEMS under an export rate to that of the HEMS under a TOU rate. The paper presents results from software simulations of a small system with multiple homes with HEMS and solar panels operating under two different tariffs: a TOU rate with net energy metering and an export rate. For the simulations, the HEMS is set up to optimize the operation of an air conditioner, water heater, and BESS to minimize the consumers' electricity bills. We use the IESM co-simulation platform to integrate the power system simulations and the HEMS.

The results reported here for a 12-home case study show that export power can be significantly increased under a TOU tariff if customers invest in BESS and associated controls, such as a HEMS, that can respond to a TOU rate. Conversely, an export tariff similar to the one studied in this paper can aid a utility in achieving an objective of reducing export power if its customers invest in a BESS and associated controls, such as a HEMS, that can respond to an export rate. We estimated energy cost savings of approximately 20% for houses with HEMS and BESS under an export rate. This is achieved through managing the charging and discharging of the BESS and by allowing the air and hot water temperatures to deviate by 2.5°F and 10°F, respectively, from the desired set point temperature.

Future work is warranted on the sensitivity of these results to the specific export rate and its relationship to the import rate. The results also show that the export rate we studied increases the electricity bill for customers with PV and that customer investment in BESS and HEMS can offset some of that increase but not all. The results also confirm earlier findings that a HEMS operating under a TOU rate can reduce the load during peak-price hours and move the load peak to hours with off-peak prices. These results point both to a need for careful design of tariff structures and to opportunities for aggregator services to coordinate loads and DERs to achieve cost savings for consumers and gain load profile improvements for utilities.

Here, we assume that the customers set the HEMS objective to be cost minimization. Results will differ if other objectives, such as greenhouse gas emissions or comfort, are included, and this warrants further study. This work presents results from a very small distribution system that is lightly loaded, and therefore we limited our analysis to total household power. Future work could simulate larger systems with many hundreds of houses and different penetrations of DERs and controls. On such a large system, analysis of the impact on the voltage (average voltages, number of voltage violations, average voltage fluctuations and voltage unbalance) across the feeder and the peak power at the feeder head, especially before and after peak prices, would be of interest. Future work to evaluate different feeders in different geographic locations can be considered as well as the extension of the HEMS to include faster (second-level) controls to reduce export power in addition to the optimization that is performed at intervals of several minutes.

ACKNOWLEDGMENT

The views expressed in the article do not necessarily represent the views of the DOE or the U.S. Government. The U.S. Government retains and the publisher, by accepting the article for publication, acknowledges that the U.S. Government retains a nonexclusive, paid-up, irrevocable, worldwide license to publish or reproduce the published form of this work, or allow others to do so, for U.S. Government purposes.

REFERENCES

[1] "Renewables 2019, market analysis and forecast from 2019 to 2024," Int. Energy Agency (IEA), Renewables Market Report, Paris, France, Tech. Rep., Oct. 2019. [Online]. Available: https://www.iea.org/reports/renewables-2019

[2] P. Frankl, "Energy system debate: What lies ahead for the future?" *IEEE Power Energy Mag.*, vol. 17, no. 2, pp. 98–100, Mar./Apr. 2019.

[3] M. S. ElNozahy and M. M. A. Salama, "Technical impacts of grid-connected photovoltaic systems on electrical networks—A review," *J. Renew. Sustain. Energy*, vol. 5, no. 3, May 2013, Art. no. 032702.

[4] P. Paudyal, P. Munankarmi, Z. Ni, and T. M. Hansen, "A hierarchical control framework with a novel bidding scheme for residential community energy optimization," *IEEE Trans. Smart Grid*, vol. 11, no. 1, pp. 710–719, Jan. 2020.

[5] R. Li, Z. Wang, C. Gu, F. Li, and H. Wu, "A novel time-of-use tariff design based on Gaussian mixture model," *Appl. Energy*, vol. 162, pp. 1530–1536, Jan. 2016.

[6] A. S. Hassan, L. Cipcigan, and N. Jenkins, "Optimal battery storage operation for PV systems with tariff incentives," *Appl. Energy*, vol. 203, pp. 422–441, Oct. 2017.

[7] A. Faruqui and C. Bourbonnais, "The tariffs of tomorrow: Innovations in rate designs," *IEEE Power Energy Mag.*, vol. 18, no. 3, pp. 18–25, May 2020.

[8] "Innovation landscape brief: Time-of-use tariffs," Int. Renew. Energy Agency (IRENA), Abu Dhabi, United Arab Emirates, Tech. Rep., Feb. 2019. [Online]. Available: https://www.irena.org/publications/2019/Feb/ Innovation-landscape-for-a-renewable-powered-future

[9] J. Sherwood, A. Chitkara, D. Cross-Call, and B. Li, "A Review of alternative rate designs: Industry experience with time-based and demand charge rates for mass-market customers," Rocky Mountain Inst., CO, USA, Tech. Rep., May 2016. [Online]. Available: http://www.rmi.org/alternative_rate_designs

[10] R. Hledik, A. Faruqui, and C. Warner. *The National Landscape of Residential ToU Rates*. The Brattle Group. Accessed: Jan. 6, 2020. [Online]. Available: https://brattlefiles.blob.core.windows.net/files/12658_the_national_landscape_of_residential_tou_rates_a_preliminary_summary.pdf

[11] U.S. Energy Information Administration. *Feed-in Tariff: A Policy Tool Encouraging Deployment of Renewable Electricity Technologies*. Accessed: Jan. 6, 2020. [Online]. Available: https://www.eia.gov/todayinenergy/detail.php?id=11471

[12] J. Tant, F. Geth, D. Six, P. Tant, and J. Driesen, "Multiobjective battery storage to improve PV integration in residential distribution grids," *IEEE Trans. Sustain. Energy*, vol. 4, no. 1, pp. 182–191, Jan. 2013.

[13] Edie. *Government Axes Renewable Feed-in Tariff Pre-Accreditation*. Accessed: Jan. 8, 2020. [Online]. Available: https://www.edie.net/news/6/Feed-in-tariff-pre-accreditation-closed-by-UK-Government-DECC/

[14] Spirit Energy. *Solar PV Export Tariffs*. Accessed: Jan. 10,2020. [Online]. Available: https://www.spiritenergy.co.uk/kb-solar-pv-export-tariff

[15] Spirit Energy. *Smart Export Guarantee Tariffs: Which is the Best Rate?*. Accessed: Jan. 10, 2020. [Online]. Available: https://blog.spiritenergy.co.uk/homeowner/smart-export-guarantee-tariffs

[16] Arizona Public Service. *Renewable Energy Riders*. Accessed: Dec. 10, 2019. [Online]. Available: https://www.aps.com/en/Residential/Service-Plans/Compare-Service-Plans/Renewable-Energy-Riders

[17] N. Martin and J. Rice, "Solar feed-in tariffs: Examining fair and reasonable retail rates using cost avoidance estimates," *Energy Policy*, vol. 112, pp. 19–28, Jan. 2018.

[18] S. Dong, E. Kremers, M. Brucoli, S. Brown, and R. Rothman, "Residential PV-BES systems: Economic and grid impact analysis," *Energy Proc.*, vol. 151, pp. 199–208, Oct. 2018.

[19] R. Khezri, A. Mahmoudi, and M. H. Haque, "Optimal capacity of PV and BES for grid-connected households in south Australia," in *Proc. IEEE Energy Convers. Congr. Expo. (ECCE)*, Sep. 2019, pp. 3483–3490.

[20] O. Talent and H. Du, "Optimal sizing and energy scheduling of photovoltaic-battery systems under different tariff structures," *Renew. Energy*, vol. 129, pp. 513–526, Dec. 2018.

[21] S. Ahmad, A. Ahmad, M. Naeem, W. Ejaz, and H. Kim, "A compendium of performance metrics, pricing schemes, optimization objectives, and solution methodologies of demand side management for the smart grid," *Energies*, vol. 11, no. 10, p. 2801, Oct. 2018.

[22] F. A. Qayyum, M. Naeem, A. S. Khwaja, A. Anpalagan, L. Guan, and B. Venkatesh, "Appliance scheduling optimization in smart home networks," *IEEE Access*, vol. 3, pp. 2176–2190, 2015.

[23] M. Beaudin, H. Zareipour, A. K. Bejestani, and A. Schellenberg, "Residential energy management using a two-horizon algorithm," *IEEE Trans. Smart Grid*, vol. 5, no. 4, pp. 1712–1723, Jul. 2014.

[24] M. Matteo and G. Rizzoni, "Residential demand response: Dynamic energy management and time-varying electricity pricing," *IEEE Trans. Power Syst.*, vol. 31, no. 2, pp. 1108–1117, Mar. 2016.

[25] M. N. Faqiry, L. Wang, H. Wu, D. Krishnamurthy, and B. Palmintier, "ADP-based home energy management system: A case study using DYNAMO," in *Proc. IEEE Power Energy Soc. Gen. Meeting (PESGM)*, Aug. 2018, pp. 1–5.

[26] T. M. Hansen, E. K. P. Chong, S. Suryanarayanan, A. A. Maciejewski, and H. J. Siegel, "A partially observable Markov decision process approach to residential home energy management," *IEEE Trans. Smart Grid*, vol. 9, no. 2, pp. 1271–1281, Mar. 2018.

[27] H. Wu, A. Pratt, and S. Chakraborty, "Stochastic optimal scheduling of residential appliances with renewable energy sources," in *Proc. IEEE Power Energy Soc. Gen. Meeting*, Jul. 2015, pp. 1–5.

[28] M. Ruth, A. Pratt, M. Lunacek, S. Mittal, H. Wu, and W. Jones, "Effects of home energy management systems on distribution utilities and feeders under various market structures," in *Proc. 23rd Int. Conf. Electr. Distrib.*, Jun. 2015, pp. 1–7.

[29] B. Sparn, D. Krishnamurthy, A. Pratt, M. Ruth, and H. Wu, "Hardware-in-the-loop (HIL) simulations for smart grid impact studies," in *Proc. IEEE Power Energy Soc. Gen. Meeting (PESGM)*, Aug. 2018, pp. 1–5.

[30] A. Pratt, M. Ruth, D. Krishnamurthy, B. Sparn, M. Lunacek, W. Jones, S. Mittal, H. Wu, and J. Marks, "Hardware-in-the-loop simulation of a distribution system with air conditioners under model predictive control," in *Proc. IEEE Power Energy Soc. Gen. Meeting*, Jul. 2017, pp. 1–5.

[31] A. J. Pimm, T. T. Cockerill, and P. G. Taylor, "Time-of-use and time-of-export tariffs for home batteries: Effects on low voltage distribution networks," *J. Energy Storage*, vol. 18, pp. 447–458, Aug. 2018.

[32] S. Ahmad, M. Naeem, and A. Ahmad, "Low complexity approach for energy management in residential buildings," *Int. Trans. Electr. Energy Syst.*, vol. 29, no. 1, p. e2680, Jan. 2019.

[33] R. Yaqub, S. Ahmad, A. Ahmad, and M. Amin, "Smart energy-consumption management system considering consumers' spending goals (SEMS-CCSG)," *Int. Trans. Electr. Energy Syst.*, vol. 26, no. 7, pp. 1570–1584, Jul. 2016.
[34] S. Ahmad, M. Naeem, and A. Ahmad, "Unified optimization model for energy management in sustainable smart power systems," *Int. Trans. Electr. Energy Syst.*, vol. 30, no. 4, Apr. 2020, Art. no. e12144.
[35] H. Ahmad, A. Ahmad, and S. Ahmad, "Efficient energy management in a microgrid," in *Proc. Int. Conf. Power Gener. Syst. Renew. Energy Technol. (PGSRET)*, Sep. 2018, pp. 1–5.
[36] S. Ahmad, M. M. Alhaisoni, M. Naeem, A. Ahmad, and M. Altaf, "Joint energy management and energy trading in residential microgrid system," *IEEE Access*, vol. 8, pp. 334–346, 2020.
[37] M. D. P. Torcellini, S. Pless, and D. Crawley, "Zero energy buildings: A critical look at the definition," Nat. Renew. Energy Lab., Golden, CO, USA, Tech. Rep. NREL/CP-550-39833, Aug. 2006. [Online]. Available: https://www.nrel.gov/docs/ fy06osti/39833.pdf
[38] S. P. D. Crawley and P. Torcellini, "Getting to net zero," *ASHRAE J.*, vol. 51, no. 9, pp. 18–25, 2009.
[39] A. Pratt, D. Krishnamurthy, M. Ruth, H. Wu, M. Lunacek, and P. Vaynshenk, "Transactive home energy management systems: The impact of their proliferation on the electric grid," *IEEE Electrific. Mag.*, vol. 4, no. 4, pp. 8–14, Dec. 2016.
[40] A. Hoke, A. Brissette, K. Smith, A. Pratt, and D. Maksimovic, "Accounting for lithium-ion battery degradation in electric vehicle charging optimization," *IEEE J. Emerging Sel. Topics Power Electron.*, vol. 2, no. 3, pp. 691–700, Sep. 2014.
[41] J. Dupačová, N. Gröwe-Kuska, and W. Römisch, "Scenario reduction in stochastic programming," *Math. Program.*, vol. 95, no. 3, pp. 493–511, 2003.
[42] D. Holmberg, M. Burns, and S. Bushby, "NIST transactive energy modeling and simulation challenge phase II final report," Nat. Inst. Standards Technol., Gaithersburg, MD, USA, Tech. Rep. 1900-603, 2019.

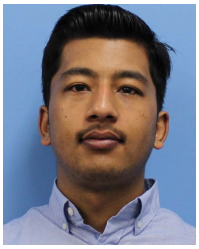

PRATEEK MUNANKARMI (Member, IEEE) received the B.E. degree in electrical engineering from Pulchowk Campus, Tribhuvan University, Kathmandu, Nepal, in 2014, and the M.S. degree in electrical engineering from South Dakota State University, Brookings, SD, USA, in 2019. He is currently a Research Engineer with the National Renewable Energy Laboratory (NREL), Golden, CO, USA. His current research interests include building energy management systems, building grid integration, and distribution system analysis.

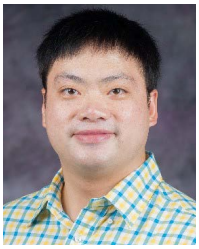

HONGYU WU (Senior Member, IEEE) received the B.S. degree in energy and power engineering and the Ph.D. degree in control science and engineering from Xi'an Jiaotong University, China. He is currently an Associate Professor and a Michelle Munson-Serban Simu Keystone Research Faculty Scholar with the Mike Wiegers Department of Electrical and Computer Engineering, Kansas State University. He was a recipient of the National Science Foundation (NSF) Career Award, the NSF EPSCoR Research Fellow, and a Team Member of the IEEE-NERC Security Integration Project. Before joining K-State, he was a Research Engineer with the National Renewable Energy Laboratory, Power Systems Engineering Center, Golden, CO, USA. His research interests include cyber-physical security of smart grids, power system planning and operation, building energy management, and grid integration of renewable energy. He is an Associate Editor of IEEE TRANSACTIONS ON SMART GRID and IEEE TRANSACTIONS ON INDUSTRIAL INFORMATICS.

ANNABELLE PRATT (Senior Member, IEEE) received the bachelor's and master's degrees in electrical and electronic engineering from the University of Stellenbosch, South Africa, and the Ph.D. degree in electrical engineering from Oregon State University. She is currently a Chief Engineer with the National Renewable Energy Laboratory, where she works on distribution management systems and microgrids; and the application of power and controller hardware-in-the-loop techniques to system performance evaluation. Prior to joining NREL, she was a Senior Power Research Engineer with Intel Laboratories. Previously, she was with Advanced Energy Industries, where she developed power supplies for the semiconductor manufacturing and architectural glass coating industries.

MONTE LUNACEK received the B.S. degree in applied mathematics from the University of Colorado at Colorado Springs, in 1998, and the M.S. and Ph.D. degrees in computer science from Colorado State University, in 2004 and 2008, respectively. He is currently a Senior Scientist with the National Renewable Energy Laboratory (NREL), where he currently uses high-performance computing and machine learning to improve transportation mobility. Prior to joining NREL, in 2014, he was a Parallel Application Developer with the University of Colorado at Boulder and a Postdoctoral Researcher at NREL, from 2009 to 2012. He was a recipient of a Parallel Problem Solving from the Nature Conference Best Paper Award, in 2006.

SIVASATHYA PRADHA BALAMURUGAN received the B.E. degree in electronics and communication engineering from Anna University, India, and the M.S. degree in computer science and engineering from University at Buffalo, SUNY. She is currently a Researcher III and a Software Engineer with the National Renewable Energy Laboratory (NREL), where she works on developing software and uses high-performance computing systems to perform simulations and hardware-in-the-loop experiments in the grid-interactive buildings and energy blockchain research areas.

PAUL SPITSEN received the bachelor's and master's degrees from the University of California at San Diego. He is currently a Technology and Policy Analyst with the Department of Energy's Strategic Analysis Team in the Office of Energy Efficiency and Renewable Energy. He focuses on cross-sectoral analysis, power sector modeling, grid integration, energy storage, and market issues.